Int. J. Electrochem. Sci., 17 **(2022)** Article Number: 220679, doi: 10.20964/2022.06.78

International Journal of ELECTROCHEMICAL SCIENCE
www.electrochemsci.org

Short Communication

Analysis of Geometric Structure, Electronic Charge Density and Absorption Spectrum of Germanium Sulfide (GeS) under an External Electric Field: A DFT calculation

XuPu Wu[1,2], *DaSen Ren*[1,*], *Lei Wu*[1]

[1] School of Mechatronics Engineering, Guizhou Minzu University, Guiyang, 550025, China.
[2] School of Physics and Electronic Sciences, Guizhou Education University, Guiyang 550018, China.
[*]E-mail: dasenren@sina.com

Received: 12 December 2021 / *Accepted:* 23 March 2022 / *Published:* 7 May 2022

The effects of an external electric field (EEF) on the properties of germanium sulfide (GeS) molecules were examined. The EEF changes the molecular electron density distribution, inducing polarization. It also induces changes in the geometric structure, especially when the EEF is large (0.0395 au). The Mayer bond level is found to be reduced. From analysis of the electron density, the EEF is found to redistribute the electron structure inside the GeS, leading to the electron to leave the domain. From excited-state calculations, the EEF is found to change the GeS excitation properties. These results are important for understanding the structural stability and design of electrodes for lithium-ion batteries based on GeS materials.

Keywords: polarization, Mayer bond level, excited state

1. INTRODUCTION

The modulation of molecular properties by an external electric field (EEF) has been extensively studied [1–5]. In general, an EEF can change the internal and external environments of a molecule, leading to changes in the physical and chemical properties, such as the molecular structure [6–12], electronic structure[13-15], and optical anisotropy [16-19]. Catalytic properties can be improved as well. Wang [20] et al. reported that an EEF can lead to hybrid reorganization of the molecular structure and result in bond cleavage. An external electric field oriented along the bond axis in a molecule will lead to significant changes in ionic properties, bond length, stretching frequency, BDE and electronic characteristics[21-22] Hence, “EEFs awaken dormant ionic structures and influence bond strengths”, as said by Thijs Stuyver[10].

GeS is a narrowband semiconductor with good optical properties and unique electronic characteristics [23-25]. The two teams of Chen Y and Chan C K showed that Ge has important application value in ion battery electrode materials for Ge-based ion batteries. [26,27] This is because germanium is 10^4 times more electronically conductive than silicon at room temperature[28] and has a 400 times higher lithium ion conduction rate than silicon[29]. Additionally, germanium has a higher multiplier performance than silicon as an anode material for use in high-power devices [30,31]. This makes GeS a promising anode material for high-power lithium-ion batteries to study the electron density and other properties of GeS under an EEF. We performed theoretical calculations to understand EEF-induced changes in GeS characteristics, especially changes in electron density.

Initially, the *ω*B97XD[30-33] density generalization in density functional theory (DFT) and the aug-cc-pvtz group were used to optimize the molecular system under an applied EEF. The calculations revealed the response of the geometric structure, electronic properties, and total energy of the system. Finally, we calculated the GeS excited states in an EEF via time-dependent DFT (TD-DFT) and produced a modulated visible-light absorption spectrum.

2. COMPUTATIONAL DETAILS

Density functional theory (DFT) is an important method for studying the electronic structure of materials [34,35]. All calculations were performed with Gaussian16[36] software with the *ω*B97XD exchange correlation functional and the aug-cc-pvtz[37] basis set. There were no imaginary frequencies in the calculations.

Table 1. Bond lengths R(Å) for GeS at different calculation levels

Method	HF exchange[a]	Basis set	R (Å)	ΔR[b]
TPSSTPSS	10%	aug-cc-pvtz	2.03178	0.01978
B3LYP	25%	aug-cc-pvtz	2.03013	0.01813
HSE06	25%	aug-cc-pvtz	2.01741	0.00541
MN15	44%	aug-cc-pvtz	1.99699	-0.01501
M06-2X	54%	aug-cc-pvtz	2.01668	0.00468
CAM-B3LYP	19%~65%	aug-cc-pvtz	2.0068	-0.0052
ωB97XD	22%~100%	aug-cc-pvtz	2.01126	-0.00074
RCCSD	-----	aug-cc-pvtz	2.01504	0.00304
UCCSD	-----	aug-cc-pvtz	2.01495	0.00295
Experimental value	-----	-----	2.012[40]	0

[a] Components of the Hartree Fock exchange functional (HFE), ~ preceded by the short-range functional and ~ followed by the long-range functional.
[b] Error between the calculated and experimental values for the GeS bond lengths at different levels

Decomposition analyses of the wave function, including the dipole moment, bond length, and Mayer bond level analysis, were performed with the Multiwfn3.8 program[38]. Based on the Gaussian output file, related parameters were extracted with Multiwfn, and the electrostatic potential distribution and the molecular volume simulation diagrams were then drawn with VMD1.9.3[39]. In the Gaussian

program, various EEF strengths (0.000−0.395 a.u.) were applied along the key axis via the keyword "field". Throughout this work, we varied the EEF in the same direction as that in the conventional physics definition. The 1 a.u value for the EEF corresponds to 51.4 V/*Å*, and 1 V/*Å* is approximately equal to 0.02 a.u.

3. RESULTS AND DISCUSSION

3.1 Study of the structural properties of germanium using density functional theory

We used various calculation methods and found that the GeS molecular bond length optimized by the ωB97XD/aug-cc-pvtz method showed the best agreement with the experimental value[40]. The error was merely 0.00074 Å. As given in Table 1, the optimized GeS bond length is closely related to the Hartree-Fock exchange functional. The error between the theoretical and experimental values of the GeS bond length decrease with increasing Hartree-Fock content, suggesting that pure general functions are not suitable for the optimization of the GeS molecules. The generalized functions of CAM-B3LYP and ωB97XD with mixed long and short ranges are more reasonable for the evaluation of the GeS structure. The advanced electronic correlation coupling cluster (CCSD) is the best method for single-configuration calculations. The results calculated with either RCCSD or UCCSD show no clear advantages over CAM-B3LYP and ωB97XD. Thus, we used ωB97XD/aug-cc-pvtz for the calculations.

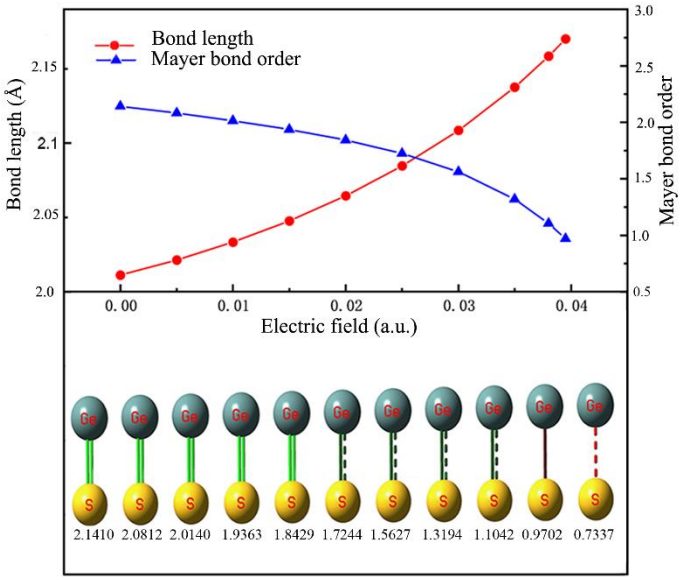

Figure 1. Bond-length and Mayer bond-level intensity changes under various external electric fields

For an EEF of 0, the GeS structural parameters were obtained through optimization. The bond length R_e of the ground state molecule is 2.01126 Å, which is consistent with the experimental value[40] of 2.012 Å. The vibrational frequency ω_e is 573.23 cm^{-1} after processing with the frequency correction factor[41]; the difference from the experimental value (575.8 cm^{-1}) is 0.32%. The EEF optimizes the GeS geometry. The response of the GeS structure to the EEF is shown in Figure 1, which plots the

changes in the bond length and Mayer bond level[42] and the bond level distribution diagram for various EEFs. Thus, the EEF can change the bond length along the axial direction. Stronger EEFs increase the bond length and weaken the bond order. This occurs because of changes in the resulting force[2] between the internal forces of the molecule and the EEF in the optimization process. This leads to the movement of charge under the resulting force and a change in bond length to optimize the geometric structure. When the electric field intensity is 0.0395 a.u., the bond-level intensity decreases to 0.7317, and the interaction between Ge and S is reduced. Hence, the bonds are barely formed. Therefore, the EEF limit is 0.0395 a.u.

We estimated the changes in the GeS molecular radius, surface area, and volume under an EEF. Table 2 indicates the relevant parameters. As the EEF is increased, the bond length, molecular radius, molecular surface area, and molecular volume all increase, which will result in more active GeS molecules.

Table 2. Molecular volume parameters under different external electric fields (EEFs)

EEF (a.u.)	Radius (Å)	Surface (Å2)	Volume (Å3)
0.000	2.906	89.68837	76.70440
0.005	2.911	89.75989	76.73672
0.01	2.917	89.94260	76.88749
0.015	2.924	90.24082	77.15907
0.02	2.932	90.67216	77.59210
0.025	2.942	91.25540	78.17996
0.03	2.954	92.02935	78.97740
0.035	2.969	93.04837	80.02889
0.038	2.979	93.81272	80.84260
0.0395	2.985	94.24565	81.29295

3.2 Stress changes for the electronic properties of GeS vs. *the action of an external electric field*

The response of a molecular system to an EEF is driven by electronic polarization, and the dipole moment is the most direct indicator of the degree of polarization. The induced dipole moment of a molecular system under an EEF can be expressed as follows:

$$\mu = \mu^0 + \alpha F + \frac{1}{2}\beta F^2 + \cdots \qquad (1)$$

Here, μ_0 is the dipole moment without an EEF, α is the dipole-moment polarization rate, and β is the first hyperpolarization rate. We focused on the contribution of the polarization rate to the dipole moment variation. As shown in Figure 2, the polarization rate change in the z-direction is higher because the applied electric field points in that direction. With increasing EEF, α_{zz} increases, which is mainly because of the change in α_{zz} caused by the excitation of bonding σ orbitals to antibonding σ* orbitals. Hence, increasing the EEF leads to frequent σ→σ* excitations and increased α_{zz}, which polarizes the molecule. Isotropic and isotropic mean polarizability volumes for different electric fields are depicted in Figure 3; as the electric field increases, both the isotropic and isotropic volumes change, but the

magnitude of the change is not large; this can enable one to avoid sharp changes in volume in a single direction and improve structural stability[43]

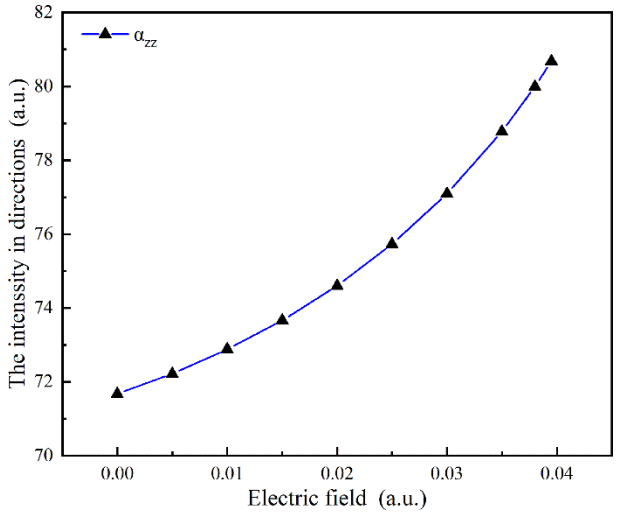

Figure 2. Changes in *z*-direction polarizability α vs. external electric field.

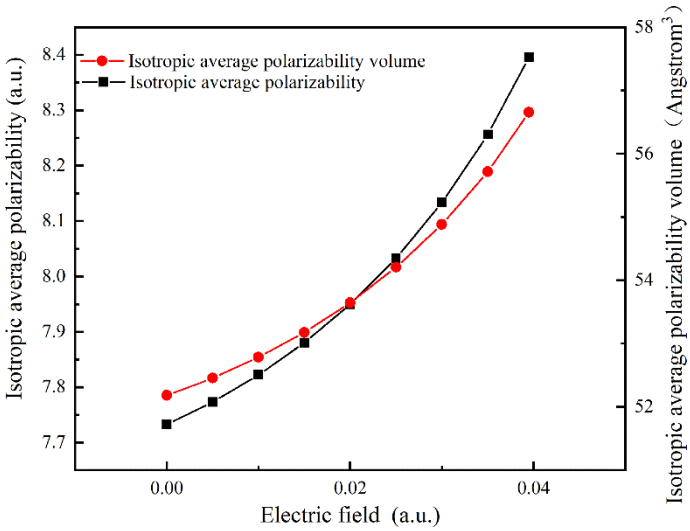

Figure 3. Isotropic average polarizability and isotropic average polarizability volume vs. external electric field.

To visualize and fully demonstrate the EEF polarization effect on GeS, we calculated the electron density difference (Δρ) before and after the application of a 0.0395 a.u. EEF. Figure 4 (a) shows the electron density map for GeS molecules without an electric field. The electron density distribution is uniform with no out-of-domain phenomena. Figure 4 (b) shows the electron density difference when the 0.0395a.u. EEF is compared with the case without an electric field. The solid line represents the region where the electron density increases in the electric field, and the dashed line represents the region where it decreases. This indicates that the electric field induces a large polarization effect on the electron density distribution. The external electric field leads to a sharp change in the electron density, indicating that under an external electric field, the electrons in GeS are obviously delocalized. This will help with the

transmission of electrons in an ion battery, increase the transmission rate of electrons and ions, and result in high rate performance while ensuring a high capacity for the electrode. [44]

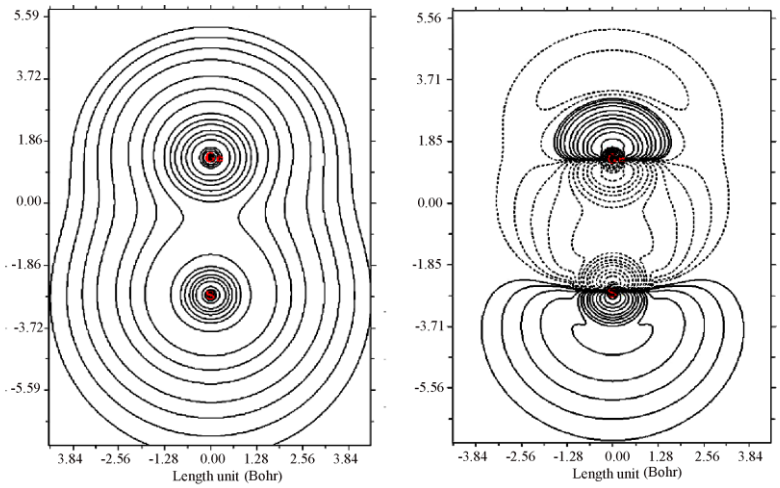

Figure 4. (a) ρ contour map when the electric field intensity is 0, and (b) the electron density difference (Δρ) after application an electric field with an intensity of 0.0395 au. The dashed line represents the reduced density and the solid line represents the increased density.

To further analyze the effect of an EEF on the polarization of GeS molecules, we selected the electrostatic potential distribution for an EEF of magnitude 0.0395 a.u. Figure 5 depicts the van der Waals surface electrostatic potential distribution of GeS molecules at the stronger EEF, with Figure 5(a) as the main view, Figure 5 (b) as the top view, and Figure 5 (c) as the bottom view. The blue- and red-colored regions correspond to negative and positive electrostatic potentials, respectively, and the locations of the maximum and minimum values of the surface electrostatic potential are indicated. The overall reorganization of the electron density leads to a distribution of the electrostatic potential of the molecule, which is significantly negative (up to −67.954429 kcal/mol) near the source of the electric field and significantly positive on the other side (up to 85.924455 kcal/mol). The change in the intramolecular electric field contributes to intramolecular charge separation and to the transfer of charge within the molecule.

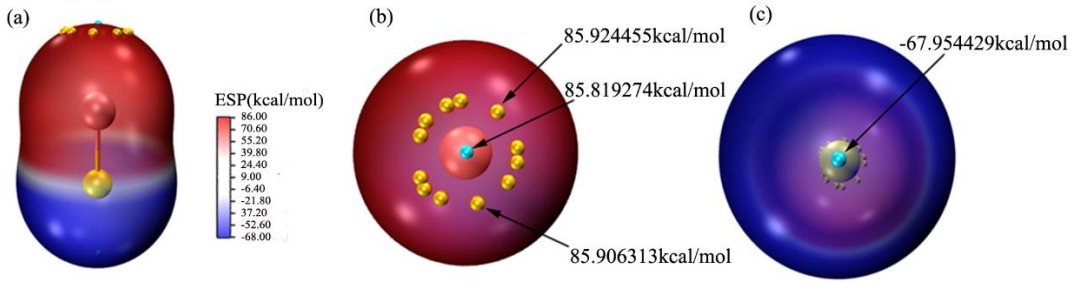

Figure 5. van der Waals surface electrostatic potential distribution for GeS molecules under a strong external electric field. (a) front view, (b) top view, and (c) bottom view.

3.3 Analysis of the energy change components

As shown in Figure 6, the effect of EEF on the total molecular energy is very significant. The increase in EEF leads to a significant decrease in the total energy, which is attributed to changes in the molecular geometry and electronic structure. There are three main reasons for this, and we decompose the energy changes into three parts, as shown in Eq. (2):

$$E\left[\psi^0(R^0),\widehat{H}^0\right] \xrightarrow{\triangle E_{der}} E\left[\psi^0(R^F),\widehat{H}^0\right] \xrightarrow{\triangle E_{int}} E\left[\psi^0(R^F),\widehat{H}^F\right] \xrightarrow{\triangle E_{relax}} E\left[\psi^F(R^F),\widehat{H}^F\right] \quad (2)$$

Here, ψ is the electronic wave function, R is the coordinate, Ĥ is the Hamiltonian, 0 represents no electric field, and F represents the applied EEF. The parameter ΔE_{der} is the energy change resulting from the EEF-induced deformation of the geometric structure. The value ΔE_{int} is the energy change due to the interaction between the permanent dipole moment of the system and the EEF-induced deformed structure. The value ΔE_{relax} is the energy change that occurs during the relaxation of the electronic structure under an EEF for the deformed structure.

The change in total energy can be expressed as follows:

$$\Delta E_{total} = E[\psi^F(R^F),H^F] - E[\psi^0(R^0),H^0] = \Delta E_{der} + \Delta E_{int} + \Delta E_{relax} \quad (3)$$

As shown in Figure 6, the black curve reflects the effect of the change in the geometric structure on the total energy of the system. This structural contribution to the total energy change is very small. The green curve indicates that the change in ΔE_{relax} is not significant for increasing EEF, and the decrease in energy due to electron relaxation is not significant. Electronic relaxation does not dominate the change in the total energy. The ΔE_{int} values (blue curve) indicate that the dipole moment induced by the EEF sharply decreases the system energy. The change in dipole moment dominates the reduction in the system energy because the polarizability greatly changes with the EEF, resulting in significant changes in the dipole moment. Therefore, it can be inferred that changes in the molecular geometry and electronic relaxation affect the total energy but are relatively weak, while the EEF-induced dipole moment does change significantly, which is the main reason for the sharp decrease in the total molecular energy. This is because, in a field-free environment, the interaction between nonpolar GeS molecules mainly involves attractive dispersion, and as the EEF increases the molecular polarization, the charge distribution changes, and the dispersion and polarization between the molecules also changes. This interaction leads to a change in the intermolecular potential of the GeS molecules, which results in a decreased interaction between induced dipoles. However, the vibrational frequency changes with the increased EEF. According to the Stark effect, the dipole moment and the polarizability significantly increases with increasing EEF, resulting in a sharp decrease in the vibrational frequency. Thus, the vibrational energy is also reduced. Hence, the decreased total energy is attributed to a decrease in electronic and vibrational energies with increasing EEF.

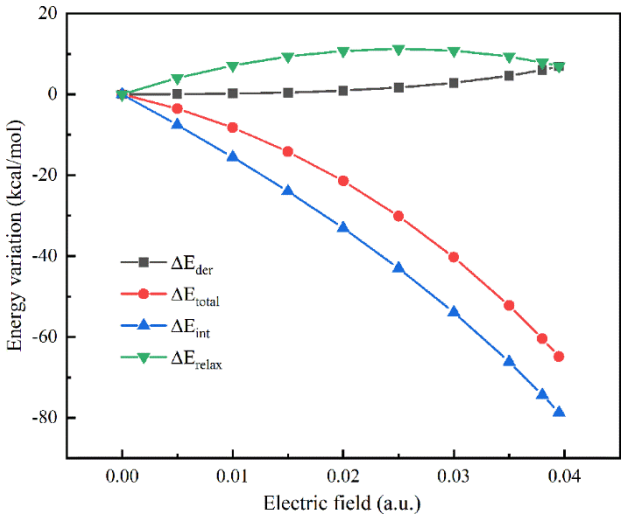

Figure 6. The effect of the external electric field on the total energy change and composition of GeS

3.4 Modulation of the GeS excitation spectrum by an external electric field

Figure 7 shows the electronic absorption spectra for GeS at different EEF intensities for excitation energies and vibronic intensities calculated via time-dependent density functional theory (TD-DFT). When the external electric field is 0–0.03 a.u., the spectral properties do not change much relative to those without the EEF. There is no absorption in the visible region, but there is a very intense absorption peak in the ultraviolet region near 150 nm, which is attributed to the jump in electron excitations from occupied to unoccupied orbitals.

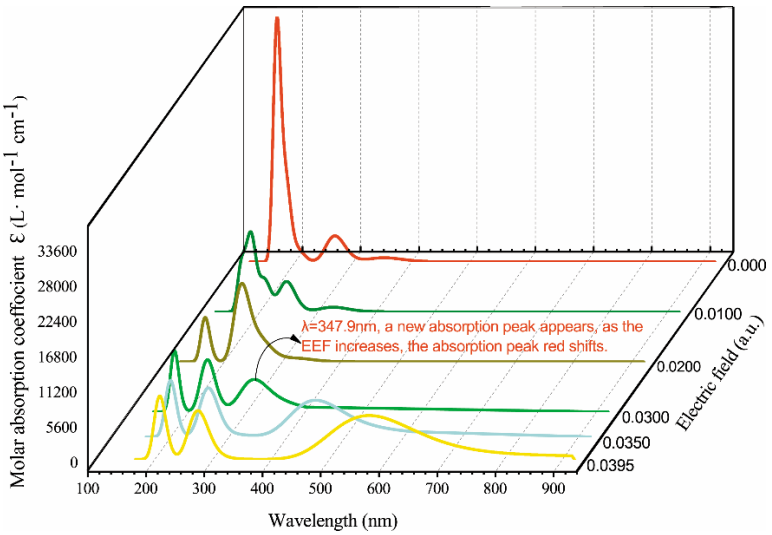

Figure 7. Effect of the modulation of external electric fields on the absorption spectrum of GeS

Figure 8 shows 5 occupied and 5 unoccupied molecular orbitals at different EEFs. The EEF effect on the energy of the highest-occupied molecular orbital (HOMO) is very weak, while a significant

decrease in the energy of the lowest unoccupied molecular orbital (LUMO) decreases the energy gap, which increases the photocatalytic hydrolysis efficiency [45].

When the EEF is increased to 0.03 a.u., the ultraviolet absorption decreases, and a significant new absorption band appears in the visible region, resulting to a redshift in the absorption edge and an expanded GeS absorption range. The wavelength of the new band and the absorption intensity both increase with the EEF, which indicates that the EEF modulates the GeS absorption and increases the photocatalytic hydrolysis efficiency. It can be predicted that the absorption capacity of the electronic spectrum will be further enhanced at large EEFs.

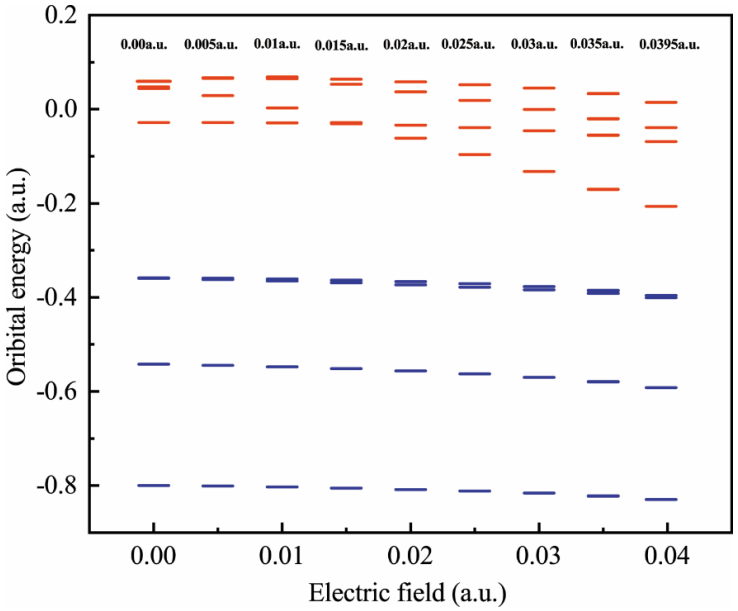

Figure 8. Distribution of occupied and unoccupied orbits under different external electric fields (EEFs)

To examine the mechanism of the new visible absorption band induced by the EEF, we used EEF=0.0395 a.u. Figure 9 decomposes the total absorption spectra and plots the contributions of the electronic excitation and the vibrational intensity for values greater than 0.1. The maximum absorption band generated by the EEF at 567.8512 nm is mainly attributed to the $S_0 \rightarrow S_2$ excitation, 98.6% of which is contributed by the HOMO-2 to LUMO transition. From the contours of the two orbitals, HOMO-2 is a σ orbital, while LUMO is a σ^*orbital. $\sigma \rightarrow \sigma^*$ excitation results in a visible absorption band. Moreover, because the LUMO is very low in the current state, the excitation energy is very low (2.1849 eV); thus, the corresponding visible absorption is decreased.

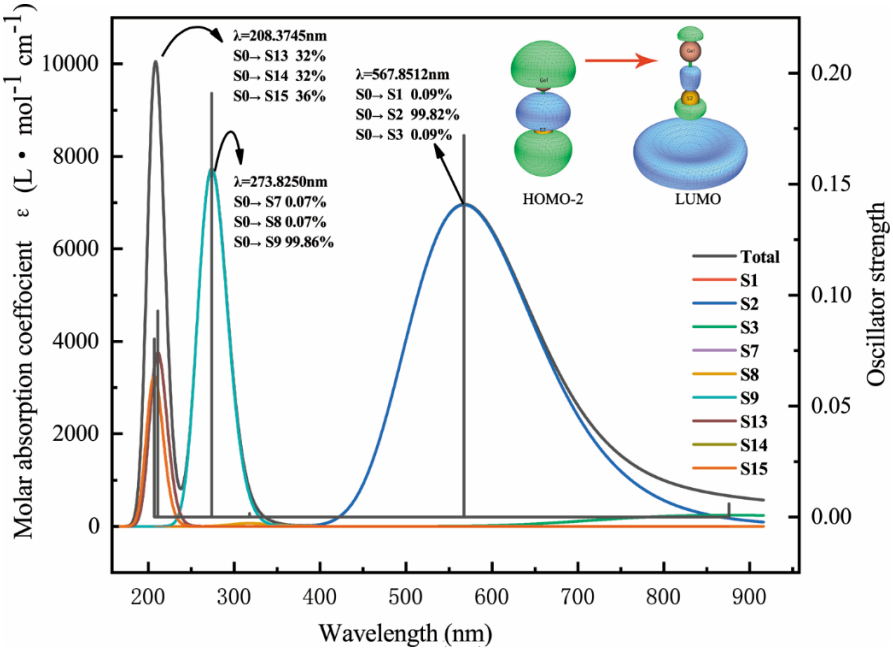

Figure 9. The electron excitation contribution curve and orbital contour map with vibrational intensity greater than 0.1 for EEF =0.0395 a.u. The maximum absorption band at 567.8512 nm is attributed to $S_0 \rightarrow S_2$ excitation. The highest-occupied molecular orbital (HOMO-2) is a σ orbital, and the lowest-unoccupied molecular orbital (LUMO) is a σ* orbital.

4. CONCLUSIONS

We examined the effects of EEFs on GeS by computational calculations. An EEF is found to induce changes in the electronic structure of the system, leading to a redistribution of charges within the molecule, which ultimately results in molecular polarization. For increasing EEF, the GeS bond length is significantly elongated in the direction of the field and the Mayer bond level is significantly weakened. In the calculated excited state, it is found that the EEF significantly increases the electronic spectrum absorption capacity of GeS. When EEF exceeds 0.02 au, molecular orbital excitations became active as the EEF is increased, weakening the strong ultraviolet absorption peak. Due to the active σ→σ* transition, the system shows a significant absorption band in the visible region, which can greatly increase the catalytic activity of GeS.

CONFLICTS OF INTEREST

There are no conflicts of interest to declare.

ACKNOWLEDGEMENTS

This work was supported by the Growth Foundation for Young Scientists of Guizhou Provincial Department of Education (Grant No. QJH KY [2018]265), the Science and Technology Planning Project of Guizhou Province (Grant No.[2018]1119), Science Foundation of Guizhou Province (Qian Ke He JiChu [2019] 1248), The Central Guiding Local Science and Technology Development Foundation of China (Grant No. QK ZYD[2019]4012)

References

1. S. D. Fried, S. Bagchi and S. G. Boxer, *Science*, 346 (2014)1510.
2. T. Lu and Q. Chen ,*Chem.Phys.Chem*, 22 (2021)386.
3. N. J. English and C. J. Waldron, *Phys.Chem.Phys.Chem*, 17 (2015) 12407.
4. J. Chen, S. Liu, M. Li, C. Rong and S. Liu, *Chem. Phy. Lett.*, 757 (2020) 137858.
5. G. Chanana and K. Batra, V. Prasad, *Comput. Theor. Chem.*, 1169 (2019) 112620.
6. L. Hao, J. Wang, D. Zhai, P. Ma, C. Ma, Y. Pan and J. Jiang, *ACS omega.*, 5 (2020) 14767.
7. J. Wu, X. Wang, Y. Ji, L. He and S. Li, *Phys. Chem.Phys.Chem.*, 18 (2016) 10309.
8. H. G. Peng, Z. Zhou, H. Merlitz and C. X. Wu, *Chem. Phys.Lett.*, 653 (2016) 196.
9. V. Enchev, V. Monev, N. Markova, M. Rogozherov, S. Angelova and M. Spassova, *Comput. Theor. Chem.*, 1006 (2013)113.
10. T. Stuyver, D. Danovich, J. Joy and S. Shaik, *Wires Comput Mol Sci.,* 10 (2020) 1438.
11. Y.H. Yin and Q. Wang, *J.Chem. Phys.*, 539(2020) 110925.
12. H. Yong snd Y. Zhao, *Int. J. Electrochem. Sci.*, 14 (2019) 8750 .
13. K. Wu, Y. Li and X. Wu, *Chem. Phys. Lett.*, 15 (2021) 138790.
14. K. Narita and S. Okada, *Chem. Phys. Lett.*, 614 (2014)10.
15. C. Yan, K. Afrasyab, T. Elham, B.Masoud,T. Baei Mohammad, M. Hossein, S. Alireza, P.Maedeh, H.N.Amir and B. Albadarin, *J.Mol. Liq.*, 340 (2021) 116845.
16. S. Shaik, R. Ramanan, D. Danovich and D. Mandal, *Chem. Soc. Rev.*, 47 (2018) 5125.
17. X. Zhang, Y. Liu, X. Ma, F. Jin, B. Abulimiti and M. Xiang, *Optik*, 221 (2020)165395.
18. Y. Tao, Q. Wang, K. Sun, Q. Zhang, W. Liu, J. Du and Z. Liu, *Spectrochim. Acta. A*, 231 (2020)118108.
19. Y. Wang, F.D. Ren and D.L. Cao, *J .Mol. Model.*, 25 (2019) 330.
20. N. Wang, K. Kaminski, J. Petera, A. M. Allgeier and L. R. Weatherley, *Chem.Eng. J.*, 374 (2019) 1096.
21. L. Rincon, J.R. Mora, F.J. Torres and R. Almeida, *Chem. Phys.*, 477 (2016)1.
22. P. Papanikolaou and P. Karafiloglou , *Theor Chem Acc*, 126(2010) 213.
23. F. Pansini, F. De Souza and C. Campos, *J Comput Chem*, 39 (2018) 1561.
24. R. K. Ulaganathan, Y. Y. Lu, C. J. Kuo, S. R. Tamalampudi, R. Sankar, K. M. Boopathi, A. Anand, K. Yadav, R. J. Mathew, C. R. Liu, F. C. Chou and Y. Chen, *Nanoscale*, 8 (2016) 2284.
25. P. Zhao, H. Yang, J. Li, H. Jin, W. Wei, L. Yu, B. Huang and Y. Dai, *J. Mat. Chem. A*, 5 (2017) 24145.
26. T. Song, H. Cheng, K. Town,H. Park, R. W. Black , S. Lee, W. I. Park, Y. Huang, J. A. Rogers, L. F. Nazar and U. Paik, *Adv. Funct. Mater.*, 24(2014)1458.
27. W. Liang, H. Yang, F. Fan, Y. Liu, X. H.Liu, J. Y. Huang, T. Zhu and S. Zhang, *ACS Nano*, 7(2013)3427.
28. C. Xilin, G. Konstantinos, G. Juchen, B. Adam, W. Chunsheng, G. Reza and N. C. James, *ACS Nano*, 4(2010)5366.
29. J. Graetz, C. C. Ahn, R. Yazami and B. Fultz, *J. Electrochem. Soc.*,1 51(2004), A698-A702.
30. X. Li, Z. Li and J. Yang, *Phys. Rev. Lett.*, 112 (2014) 018301.
31. M. Malik and D. Michalska, *Spectrochim. Acta. A.*, 125 (2014)431.
32. D. Jacquemin, E. A. Perpete, I. Ciofini and C. Adamo, *Theo.Chem.Acc*., 128 (2011) 127.
33. J. D. Chai and M. Head-Gordon, *Phys.Chem.Chem.Phys.*, 10 (2008) 6615.
34. S. Khan, A. Obaid, L. Alharbi, M. Arshad and A.M. Asiri, *Int. J.Electrochem. Sci.*, 10 (2015) 2306-2323.
35. F. X. Chen1 and L. B. Yu, et al., *Int. J.Electrochem. Sci.*, 16 (2021)1.
36. M. Frisch, G. Trucks, H. Schlegel, G. Scuseria, M. Robb, J. Cheeseman, G. Scalmani, V. Barone, G. Petersson and H. Nakatsuji, et al., *Gaussian,* 16 (2016).
37. A. D. Becke, *J.Chem.Phys.*, 107(1997) 8554.
38. T. Lu and F. Chen, *J. Comput. Chem*., 33 (2012) 580.

39. W. Humphrey, A. Dalke and K. Schulten, *J. Mol. Graph. Model.*, 14 (1996) 33.
40. K. Hubert, G. Herzberg, *Molecular spectra and molecular structure constants of diatomic molecules*, Springer, (1979) New York,US.
41. R. D. J. III, Nist computational chemistry comparison and benchmark database nist standard reference database, *http://cccbdb.nist.gov/vibscalejust.asp*, 2021.
42. I. Mayer, Charge, bond order and valence in the ab initio scf theory, *Chem. Phys. Lett.*, 97 (1983) 270.
43. B. Kang and G. Ceder, *Nature*, 458 (2009)190.
44. W. Xiao, J. Zhou, L. Yu, L. J. Chen and C.W.Liu, *Angew. Chem. Int. Ed.*, 55 (2016) 7427.
45. S. Manzetti, T. Lu, H. Behzadi, M. D. Estrafili, H.L. T. Le and H.Vach, *RSC advances*, 5 (2015) 78192.